

# Characteristics of Impulsive Noise in the 450-MHz Band in Hospitals and Clinics

T. Keith Blankenship, *Student Member, IEEE*, and Theodore S. Rappaport, *Senior Member, IEEE*

**Abstract**—This paper presents an experimental study of impulsive noise in urban hospitals and clinics. A receiver was designed to resolve impulsive noise bursts as short as 2  $\mu$ s in duration in the 450-MHz band. Extensive measurements were taken at three hospitals and three clinics in three major urban areas across the United States and empirical models are provided for the amplitude, interarrival time, and duration distributions of observed impulsive noise events. This work may be used in modeling the noise found in indoor wireless communication channels.

**Index Terms**—Impulse noise, indoor radio communication.

## I. INTRODUCTION

WIRELESS links may be adversely affected by the channel through which the radio frequency (RF) signal must propagate. One particularly detrimental characteristic of the channel is the presence of ambient electromagnetic noise, which is often produced by various electrical devices. The electromagnetic fields radiated by these interfering devices may be received as spurious signals and, hence, are a source of noise.

Such noise is often impulsive in nature and is thus distinguished from the thermal Gaussian noise produced in the receiver system itself. A simple base-band model of impulsive noise is provided in Fig. 1, which shows the random nature of the amplitude, interarrival time, and duration of impulsive noise bursts. Impulsive noise is often more important to determining system degradation than Gaussian noise, especially at VHF frequencies and higher [1]. Examples of impulsive noise sources previously investigated include automobile ignitions [2], [3], microwave ovens [4], [5], photocopier machines [5], fluorescent lights [6], and power lines [6].

Previous research into electromagnetic compatibility issues in the 450-MHz band in hospitals [7]–[11] have mainly focussed on measurements and/or predictions of average ambient electric field strengths. However, we are not aware of any studies to date on the amplitude and time characteristics of impulsive noise bursts in hospitals and clinics.

This paper presents a thorough study of impulsive noise in the 450-MHz band in hospitals and clinics. It begins by describing the experimental apparatus constructed to resolve and measure individual noise bursts as short as 2  $\mu$ s in duration. Next, the series of impulsive noise measurements at three hospitals and three clinics in three major urban areas

Manuscript received June 4, 1996; revised March 5, 1997.

The authors are with the Mobile and Portable Radio Research Group, Bradley Department of Electrical and Computer Engineering, Virginia Polytechnic Institute and State University, Blacksburg, VA 24061 USA.

Publisher Item Identifier S 0018-926X(98)01487-2.

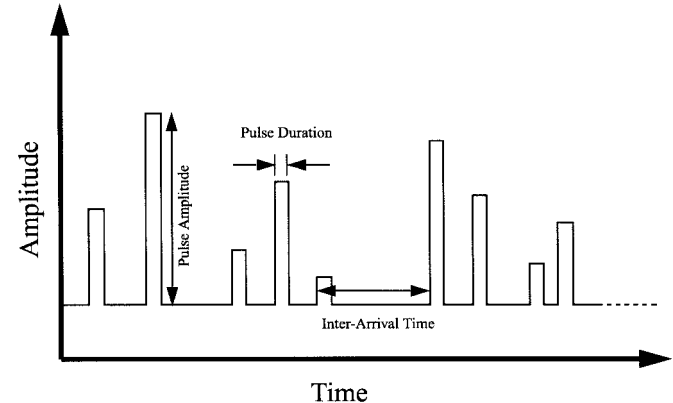


Fig. 1. A simple base-band model of impulsive noise.

across the United States is described. This is followed by a discussion of the methods by which the amplitude, interarrival time, and duration distributions of the observed impulsive noise bursts were determined from the experimental data. The experimental results on these distributions are presented and this paper concludes with a summary of these results and suggestions for future studies on impulsive noise in hospitals and clinics.

## II. EXPERIMENTAL METHODS

### A. Experimental Apparatus

Fig. 2 shows the impulsive noise measurement system. The ambient impulsive noise was captured by a quarterwave monopole antenna magnetically mounted on a ground plane. The antenna was “tuned” by trimming it to the length at which the return loss measured at 450 MHz was maximized. The front-end tunable bandpass filter had a 3-dB bandwidth of approximately 20 MHz and was used to limit the amount of energy which was allowed to pass into the amplifier. The insertion loss of the bandpass filter was measured to be approximately 1 dB, thus

$$G_f = 0.79 (=) -1 \text{ dB}$$

and

$$F_f = 1.26 (=) 1 \text{ dB}$$

where  $G_f$  is the filter gain and  $F_f$  is the filter noise figure.

The amplifier (Mini-Circuits ZFL-1000H) had a power gain  $G_{\text{amp}}$  of

$$G_{\text{amp}} = 2512 (=) 34 \text{ dB}$$

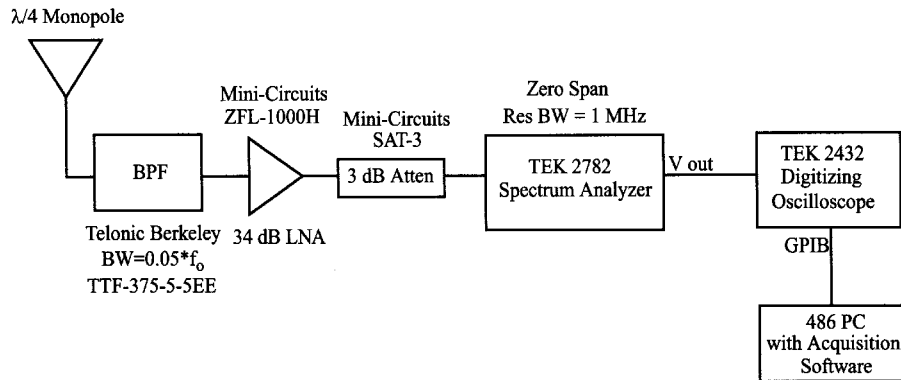


Fig. 2. The receiver and data acquisition systems used for impulsive noise measurements.

and a noise figure  $F_{\text{amp}}$  of

$$F_{\text{amp}} = 2.96 (=) 4.72 \text{ dB.}$$

An attenuator having gain  $G_{\text{att}}$  and noise figure  $F_{\text{att}}$  of

$$G_{\text{att}} = 0.5 (=) -3 \text{ dB}$$

and

$$F_{\text{att}} = 2 (=) 3 \text{ dB}$$

was placed after the amplifier to absorb any power reflections within the system and to reduce the overall gain of the radio frequency (RF) front end to 30 dB. The bandpass filter, amplifier, and attenuator were mounted on a rigid steel plate along with a 15-V linear shielded power supply. The components were interconnected using SF-142B coaxial cable.

The spectrum analyzer was placed in zero span mode at a frequency (nominally 440 MHz) where activity in the spectrum was deemed to be free of coherent interference (e.g., pager transmitters). The resolution bandwidth of the spectrum analyzer was set to 1 MHz, which, being the smallest bandwidth of any filter in the system, was identified as the system bandwidth. With an RF system bandwidth of 1 MHz, a noise pulse with a base-band bandwidth of 500 kHz or a time duration of 2  $\mu$ s was the shortest pulse that could be resolved.

The signal at the "V out" (vertical deflection) port of the spectrum analyzer (see Fig. 2) was the output of an internal log amplifier detector. The voltage at this port was proportional to the logarithm of the power contained in the passband of the resolution bandwidth filter of the spectrum analyzer. This signal was sampled and quantized using a Tektronix 2432 digitizing oscilloscope running in envelope mode, which captured the peak voltages in 512 equally spaced consecutive bins over time.

The spectrum analyzer was found to have a noise figure  $F_s$  of

$$F_s = 794 (=) 29 \text{ dB.}$$

Using the values of the gain and noise figure of all devices in the system, a theoretical value for the composite noise figure of the system  $F_{\text{sys}}$  was determined from (1) to be 6.6 dB

$$F_{\text{sys}} = F_f + \frac{F_{\text{amp}} - 1}{G_f} + \frac{F_{\text{att}} - 1}{G_f G_{\text{amp}}} + \frac{F_s - 1}{G_f G_{\text{amp}} G_{\text{att}}} = 4.54 (=) 6.6 \text{ dB.} \quad (1)$$

Since the RF bandwidth of the system was 1 MHz, only received pulses of 2  $\mu$ s or longer could pass through the system without significant distortion. Thus, the oscilloscope sweep speed was set such that the duration of a time bin was equal to the minimum resolvable pulse duration of 2  $\mu$ s, which corresponded to a sweep speed of 50  $\mu$ s/div. Data were also collected using oscilloscope sweep speeds of 5 ms/div and 500 ms/div for minimum resolvable pulse durations of 200  $\mu$ s and 20 ms, respectively. This was done to ensure that significant impulsive noise bursts were not overlooked during the "dead time" in which the oscilloscope rearmed its trigger circuits after completing a sweep. Data taken at sweep speeds of 5 ms/div also proved to be beneficial for observing the impulsive noise produced by 60-Hz interferers.

The trigger level of the oscilloscope was set manually so that it would be triggered by impulsive noise rather than by thermal noise. Although the exact level varied from run to run, it was found that a level of 27 to 34 dB above  $kT_0 B$  was sufficient for this purpose. During typical runs the oscilloscope triggered at a rate of two or three times per second. The trigger offset was set such that the first tenth of a sweep was captured prior to the trigger pulse, while the remaining nine-tenths of the sweep were captured after the occurrence of the trigger pulse. Following each oscilloscope sweep and acquisition the envelope was refreshed in preparation for the next sweep. The oscilloscope settings were adjusted to ensure that the full dynamic range of impulsive noise voltages could be captured.

The Tektronix 2432 quantized the peak input voltages in 512 consecutive time bins to one of 256 integer values. A data acquisition system using the National Instruments general purpose interface board (GPIB) data acquisition hardware and software was used to acquire the data from each oscilloscope sweep. The quantized values of each oscilloscope sweep were time stamped and written to computer hard disk for off-line processing. A total of 224 oscilloscope sweeps were recorded for each run of the measurement system.

The quantized output voltages were converted into absolute power referred to the antenna terminals by calibrating the system at the start of each measurement run. This calibration was accomplished by introducing a continuous wave (CW) signal of a known power into the system at the antenna terminals and varying this power between -110 and -30 dBm in 10-dB increments. For each input power level an

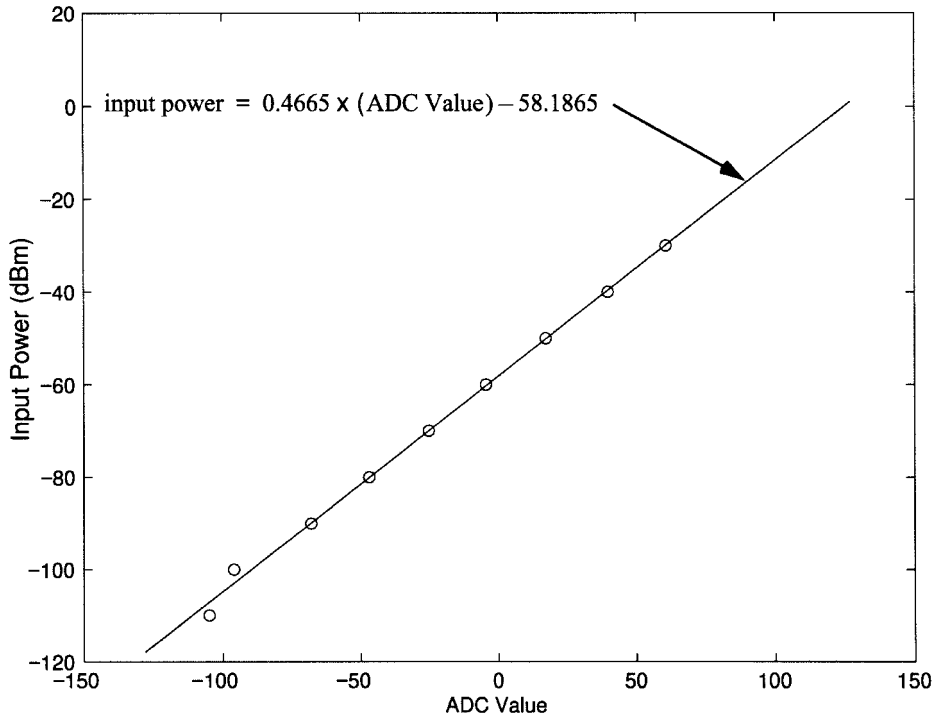


Fig. 3. Data from a typical calibration run and a regression line. The circles show the average voltage quantization level for each input power. The solid line is the result of a linear regression performed on the data.

oscilloscope sweep acquired the quantized voltages over time in a normal fashion. In subsequent off-line processing the quantized voltages produced by the input CW were averaged to obtain a single quantization level corresponding to each input power level. A linear regression, where input power was the dependent variable and average output quantization level was the independent variable, was then performed to obtain an equation capable of calculating input power in terms of voltage quantization level. The regression equation was used to convert all data acquired from the oscilloscope (expressed in voltage quantization level number) into absolute power referred to the antenna terminals.

Typical calibration data and the associated regression line are shown in Fig. 3. In general, it was consistently found throughout the measurement campaign that a change of about 0.5 dB in input power corresponded to a change of one quantization level at the output. This implies that the determination of the absolute input power was accurate to about 0.5 dB.

In addition to calibration runs and impulsive noise measurement runs at each measurement site, several runs with a  $50\Omega$  dummy load in place of the antenna were taken. For these runs the oscilloscope was allowed to trigger continuously without refreshing the envelope. After 20 s, the average voltage was read out of the oscilloscope. It was found that the average oscilloscope voltage recorded in this manner was consistently about  $-220$  mV, which corresponded to an input power of roughly  $-108$  dBm. Since the bandwidth  $B$  of the system was 1 MHz, the thermal noise power  $N$  over this 1-MHz bandwidth was

$$N = 10 \log(kT_0 B) = -114 \text{ dBm} \quad (2)$$

where  $T_0 = 290$  K has been used. Thus, the system noise

figure, being the difference between the thermal noise floor and the output noise power produced by a matched load, was consistently measured to be 6 dB. This result compares favorably with the theoretical value of the noise figure (6.6 dB), which was found above using the values of the gains and noise figures of the RF devices in the impulsive noise measurement system.

#### B. Measurement Campaign

Measurements were performed in three hospitals and three clinics in three major urban areas. The measurements in hospitals were made in procedure rooms which varied in size between  $18 \times 22$  square ft and  $21 \times 27$  square ft. The rooms were all partitioned by lead-lined walls overlaid with Sheetrock, filled with typical electronic medical equipment, and lighted with industrial standard fluorescent lighting and fixtures. One of the rooms was located on the ground floor of the hospital, another was located on the second floor, and another was located on the sixth floor. The impulsive noise measurement runs were taken under a variety of conditions in order to obtain a complete statistical sample of noise data. Some of the runs were taken when the room was inactive. Other runs were taken when technicians operated the machinery in a standard but deliberate manner to obtain noise statistics from equipment likely to produce large numbers of impulsive noise events. Still other runs were taken during actual medical procedures.

The measurements in clinics were performed in hallways and examination rooms. In general, the clinics were partitioned into small rooms by Sheetrock walls and were lighted with industrial standard fluorescent lights and fixtures. Two clinics were on ground floors, one was on the second

floor, and one clinic was on the sixth floor. The data were collected under varying levels of activity within the clinics. Some data were collected when the clinics were very busy, while other data were collected when the clinics had very few patients or activity.

Runs were taken several times throughout the day, typically, once in the morning, once at midday, and once in the late afternoon. For a data collection run a spectrum scan was first performed to identify a 1-MHz region which was devoid of any coherent interference. The center frequency of this 1-MHz region was chosen as the center frequency of the impulsive noise measurement system. Next, the receiver was calibrated according to the procedure outlined in Section II-A, followed by a run with a 50- $\Omega$  dummy load. After that, an impulsive noise data collection run with an oscilloscope sweep speed of 50  $\mu$ s/div was performed, followed by a run using an oscilloscope sweep speed of 5 ms/div. A typical run at these sweep speeds took about 3 to 5 min to complete. Runs taken at oscilloscope sweep speeds of 500 ms/div required approximately 1 h to complete and, therefore, were not performed as often.

The quarterwave monopole antenna was always mounted on a ground plane in vertical polarization. The antenna was placed either on a table or chair in the center of the room or near a wall at the side of the room. The antenna height was varied between two and eight feet above the floor.

Throughout the measurement campaign a total of 17 runs (ten at hospitals, seven at clinics) using an oscilloscope sweep speed of 50  $\mu$ s/div were performed, a total of 17 runs (ten at hospitals, seven at clinics) using an oscilloscope sweep speed of 5 ms/div were performed, and a total of three runs (one at a hospital, two at clinics) using an oscilloscope sweep speed of 500 ms/div were performed. Thus, for the minimum resolvable pulse duration of 2  $\mu$ s (50  $\mu$ s/div oscilloscope sweep speed) a total of 2240 oscilloscope sweeps were taken at hospitals and a total of 1568 oscilloscope sweeps were taken at clinics.

### III. DATA ANALYSIS

The data collected in the measurement campaign were subjected to a rigorous analysis in which the amplitude and time characteristics exhibited by the impulsive noise were quantified. All data were first calibrated according to the procedure outlined in Section II-A to convert the peak voltage in each time bin into an absolute power level. Next, the amplitude in each time bin was referenced to the thermal noise floor (-114 dBm) so that the results could be interpreted independently of the characteristics of the impulsive noise measurement system.

Fig. 4 illustrates a waveform of received power. The digitizing oscilloscope sampled the waveform at intervals of  $\tau_b$ . The peak voltage in each of 512 time bins was quantized to one of 256 levels.

A noise burst was defined as a group of one or more adjacent bins where the power in each bin exceeded a predefined threshold. For the analysis presented in this report, the threshold for each waveform was set at 6 dB above the average (in dB)

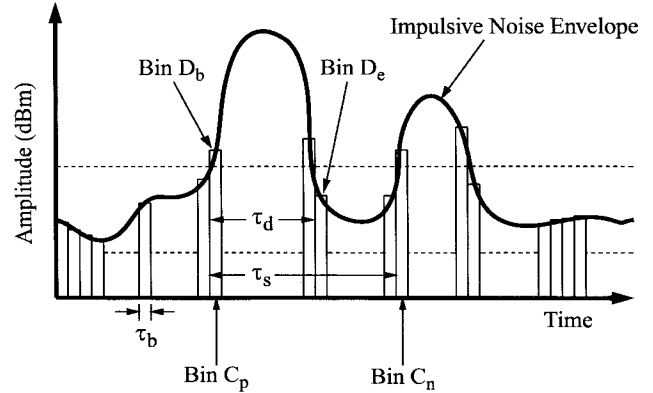


Fig. 4. An envelope of received power as might have been recorded by the measurement system. The analog waveform out of the spectrum analyzer is sampled and quantized by the oscilloscope. The output is the maximum received power in each of 512 time bins and the analog voltages are quantized to one of 256 different levels.

of the amplitude samples of the waveform. This proved to be sufficient to capture large noise bursts while simultaneously excluding effects actually due to large fluctuations of the thermal noise floor.

The quantities of interest for noise bursts are their interarrival times and their durations. As can be seen in Fig. 4, the duration of a noise burst is determined by counting the number of bins for which the noise burst exceeds the threshold. If the bin number for which the noise burst first exceeds the threshold is  $D_b$  and the bin number for which the noise burst next drops below the threshold is  $D_e$ , then the noise burst is defined as having a time duration of  $\tau_d = (D_e - D_b)\tau_b$ .

The interarrival time between two consecutive noise bursts is found as follows. If the bin number for which an arbitrary noise burst first exceeds the threshold is  $C_p$  and the bin number for which the next consecutive noise burst exceeds the threshold is  $C_n$ , then the interarrival time between the two noise bursts is defined as  $\tau_s = (C_n - C_p)\tau_b$ .

The strength of the impulsive noise was gauged by determining the amplitude probability distribution APD( $P_0$ ) of the impulsive noise [6], [12]. This is the probability that the received power from impulsive noise exceeds a particular value  $P_0$  or

$$APD(P_0) = 1 - CDF(P_0) \quad (3)$$

where  $CDF(P_0)$  is the cumulative distribution function of the amplitude of the impulsive noise.  $APD(P_0)$  was determined experimentally by counting the number of time bins in which the peak amplitude exceeded the value  $P_0$  and dividing this by the total number of time bins over which the impulsive noise was observed.

The frequency of noise bursts was gauged by determining the interarrival or pulse-spacing distribution  $PSD(\tau_s)$  [6], [12]. This is the probability that the time between two arbitrary consecutive noise bursts exceeds a particular value  $\tau_s$  or

$$PSD(\tau_s) = 1 - CDF(\tau_s) \quad (4)$$

where  $CDF(\tau_s)$  is the cumulative distribution function of the time between two arbitrary consecutive noise bursts.

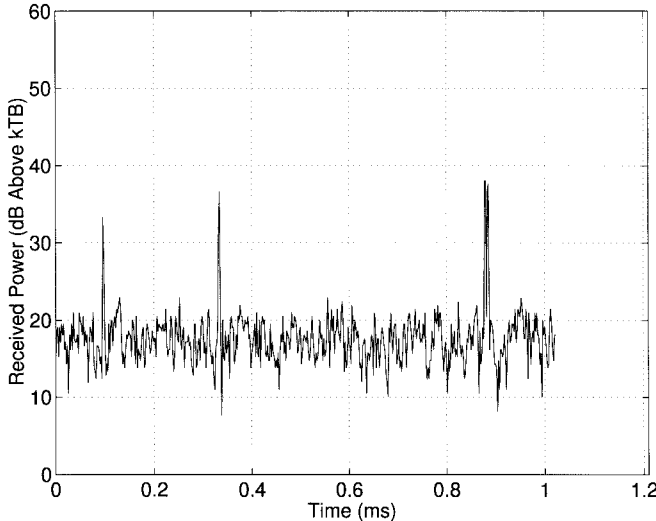


Fig. 5. An impulsive noise waveform taken using an oscilloscope sweep speed of  $50 \mu\text{s}/\text{div}$ .

Experimentally,  $\text{PSD}(\tau_s)$  was determined by counting the number of times the spacing between two consecutive noise bursts exceeded the time  $\tau_s$  and dividing this by the total number of consecutive noise bursts observed.

The duration of noise bursts was gauged by determining the pulse duration distribution  $\text{PDD}(\tau_d)$  [6], [12]. This is the probability the the duration of an arbitrary noise burst exceeds a particular value  $\tau_d$  or

$$\text{PDD}(\tau_d) = 1 - \text{CDF}(\tau_d) \quad (5)$$

where  $\text{CDF}(\tau_d)$  is the cumulative distribution function of the time duration of an impulsive noise burst. Experimentally,  $\text{PDD}(\tau_d)$  was determined by counting the number of noise bursts having durations exceeding the time  $\tau_d$  and dividing this by the total number of noise bursts observed.

These three distributions were first determined on a run-by-run basis. Then the data were combined and analyzed on a site-by-site basis. Finally, the distributions were determined for all hospitals and all clinics separately. Next, we present results on a site-by-site basis and for all hospitals and all clinics separately.

#### IV. MEASUREMENT RESULTS

##### A. General Observations

Figs. 5 and 6 show two impulsive noise waveforms recorded with an oscilloscope sweep speed of  $50 \mu\text{s}/\text{div}$ . Fig. 5 shows four distinct impulsive noise bursts (the first and second are spaced by about  $220 \mu\text{s}$ , the second and third are spaced by about  $500 \mu\text{s}$ , and the third and fourth are spaced by about  $60 \mu\text{s}$ ). Fig. 6 shows a rapid succession of impulsive noise bursts.

Figs. 7 and 8 show two impulsive noise waveform recorded with an oscilloscope sweep speed of  $5 \text{ ms}/\text{div}$ . Fig. 7 shows two medium amplitude bursts spaced about  $50 \text{ ms}$  apart, and Fig. 8 shows a succession of noise bursts spaced  $16 \text{ ms}$  apart, which is a frequency of  $60 \text{ Hz}$ .

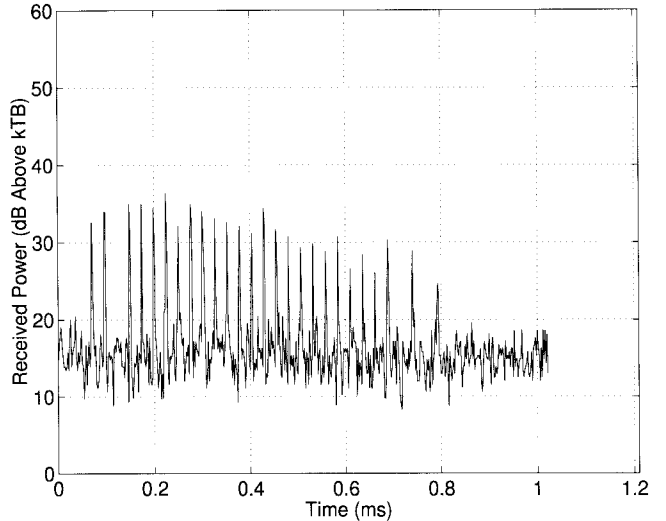


Fig. 6. An impulsive noise waveform taken using an oscilloscope sweep speed of  $50 \mu\text{s}/\text{div}$ .

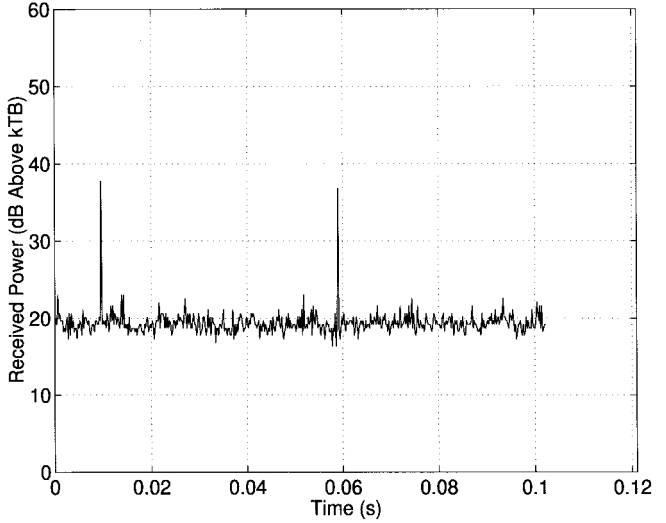


Fig. 7. An impulsive noise waveform taken using an oscilloscope sweep speed of  $5 \text{ ms}/\text{div}$ .

In general, it was found that many impulsive noise bursts were triggered by human activity within the room or by the switching of electrical or electromechanical equipment within the room. The level of impulsive noise activity did not appear to be dependent upon the time of day during which data were taken and measurements were made throughout the day at all locations. The runs taken using an oscilloscope sweep speed of  $5 \text{ ms}/\text{div}$  were useful for identifying the presence of  $60\text{-Hz}$  noise sources, as shown in Fig. 8.

##### B. Impulsive Noise Amplitude Probability Distributions

Fig. 9 shows the amplitude probability distribution observed at each individual hospital measurement site and Fig. 10 shows the amplitude probability distribution observed at each individual clinic measurement site. These distributions were observed using an oscilloscope sweep speed of  $50 \mu\text{s}/\text{div}$ , which provided a time bin duration (or sampling period) of  $2 \mu\text{s}$ . In Figs. 9 and 10 the theoretical dummy load-noise

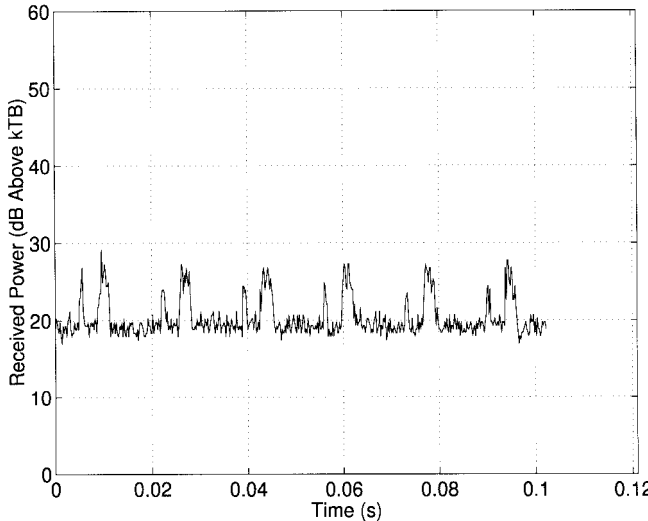


Fig. 8. An impulsive noise waveform taken using an oscilloscope sweep speed of 5 ms/div. This setting proved to be useful for the identification and observation of 60-Hz noise sources as seen in this plot.

TABLE I  
AMPLITUDES (IN DECIBELS ABOVE  $kT_0 B$ ) FOR WHICH THE AMPLITUDE PROBABILITY DISTRIBUTION IS 0.5 (MEDIAN),  $10^{-2}$  (1%), AND  $10^{-4}$  (0.01%)

Site	Median Probability	1% Probability	0.01% Probability
All Hospitals	18.3	31.1	53.0
All Clinics	14.3	35.0	56.4
All Sites	17.1	32.9	55.0

distribution due solely to thermal noise (which is Rayleigh in nature due to the envelope detection methods of the measurement system) is also plotted. In Fig. 11, the distributions from the combined data for all hospitals and clinics are plotted, along with the distribution due solely to thermal noise. The data plotted in Fig. 11 are summarized in Table I, where the values of the amplitude  $P_0$  for which  $APD(P_0)$  is 0.5,  $10^{-2}$ , and  $10^{-4}$  are given. Table I also summarizes the amplitude probability distribution for all data.

The median probability is a close approximation to the channel noise factor [6], which is the average ambient noise above thermal noise present at the antenna terminals in a given environment. Notice that the channel noise factor in hospitals is somewhat larger than that in clinics. It is likely that the leaded walls in hospitals as compared to the standard sheetrock construction of clinics plays an important role in defining observed noise levels. Also notice that the variation of the distributions among the sites is much greater for clinics than for hospitals, which seem to represent a more homogeneous statistical sample.

### C. Noise Burst Interarrival Time Distributions

Fig. 12 shows the noise-burst interarrival time probability distributions for each individual hospital measurement site as well as the combined distribution for all hospital measurement sites. Fig. 13 shows the noise-burst interarrival time probability distributions for each individual clinic measurement site as well as the combined distribution for all clinic measurement sites. These distributions were observed using an oscilloscope

TABLE II  
INTERARRIVAL TIMES (IN MICROMETERS) FOR WHICH THE INTERARRIVAL TIME PROBABILITY DISTRIBUTION IS 0.5 (MEDIAN),  $10^{-2}$  (1%), AND  $10^{-4}$  (0.01%)

Site	Median Probability	1% Probability	0.01% Probability
All Hospitals	30	720	920
All Clinics	30	650	900
All Sites	30	700	910

TABLE III  
NOISE-BURST DURATIONS (IN MICROMETERS) FOR WHICH THE NOISE-BURST DURATION PROBABILITY DISTRIBUTION IS 0.5 (MEDIAN),  $10^{-2}$  (1%), AND  $10^{-4}$  (0.01%)

Site	Median Probability	1% Probability	0.01% Probability
All Hospitals	2	16	190
All Clinics	2	44	260
All Sites	2	30	240

sweep speed of  $50 \mu\text{s}/\text{div}$ , which provided a time bin width (or sampling period) of  $2 \mu\text{s}$ . The data plotted in Figs. 12 and 13 are summarized in Table II, where the values of the interarrival time  $\tau_s$  for which  $PSD(\tau_s)$  is 0.5,  $10^{-2}$ , and  $10^{-4}$  are given. Table II also summarizes the interarrival time probability distribution for all data.

### D. Noise-Burst Duration Probability Distributions

Fig. 14 shows the noise-burst duration probability distributions for each individual hospital measurement site as well as the combined distribution for all hospital measurement sites. Fig. 15 shows the noise-burst duration probability distributions for each individual clinic measurement site as well as the combined distribution for all clinic measurement sites. The data in these distributions were observed using an oscilloscope sweep speed of  $50 \mu\text{s}/\text{div}$ , which provided a time bin width (or sampling period) of  $2 \mu\text{s}$ . The data plotted in Figs. 14 and 15 are summarized in Table III, where the values of the noise-burst duration  $\tau_d$  for which  $PDD(\tau_d)$  is 0.5,  $10^{-2}$ , and  $10^{-4}$  are given. Notice that like the amplitude probability distributions, the variation in the noise-burst duration probability distributions is much greater among the clinics as compared to the variation among the hospitals.

## V. SUMMARY AND CONCLUSION

We have presented here what we believe to be the first study of its kind of impulsive noise in hospital and clinic environments. Impulsive noise data were collected in hospital procedure rooms and clinics in three major urban areas across the United States. The data were taken under a wide variety of circumstances and, hence, should provide a good statistical sample of the impulsive noise environment in those hospitals and clinics. The system used to make the measurements was capable of resolving noise bursts of durations as short as  $2 \mu\text{s}$ , which represents a pulse with a base-band bandwidth of 500 kHz.

The data were analyzed by finding the amplitude, interarrival time, and duration distributions of the observed noise bursts. In general, the distributions in clinics were found to have a much larger variation than the distributions in hospitals,

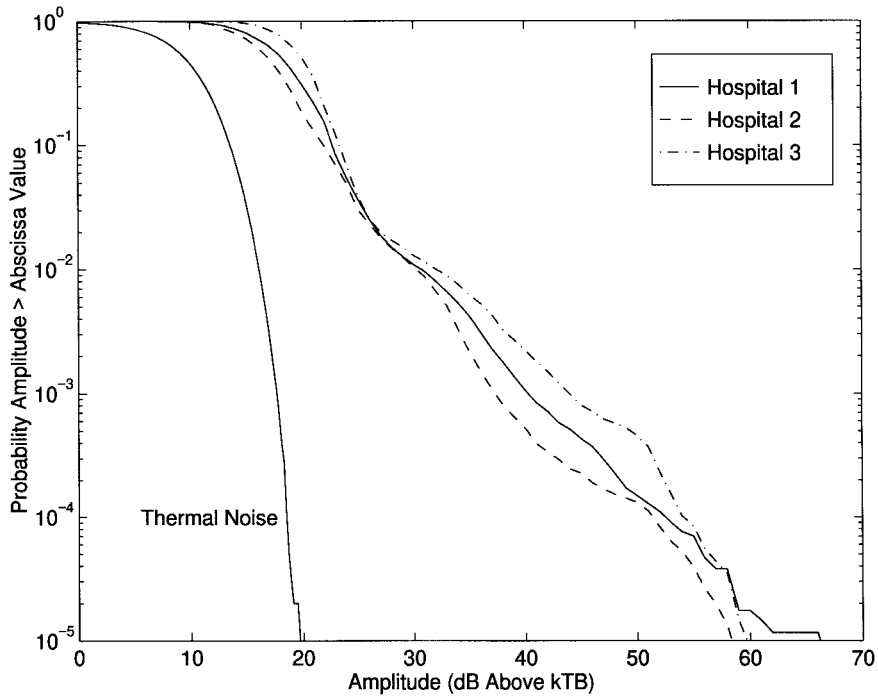


Fig. 9. The amplitude probability distribution  $APD(P_0)$  for individual hospital sites. The thermal noise distribution (labeled) is shown for comparison purposes.

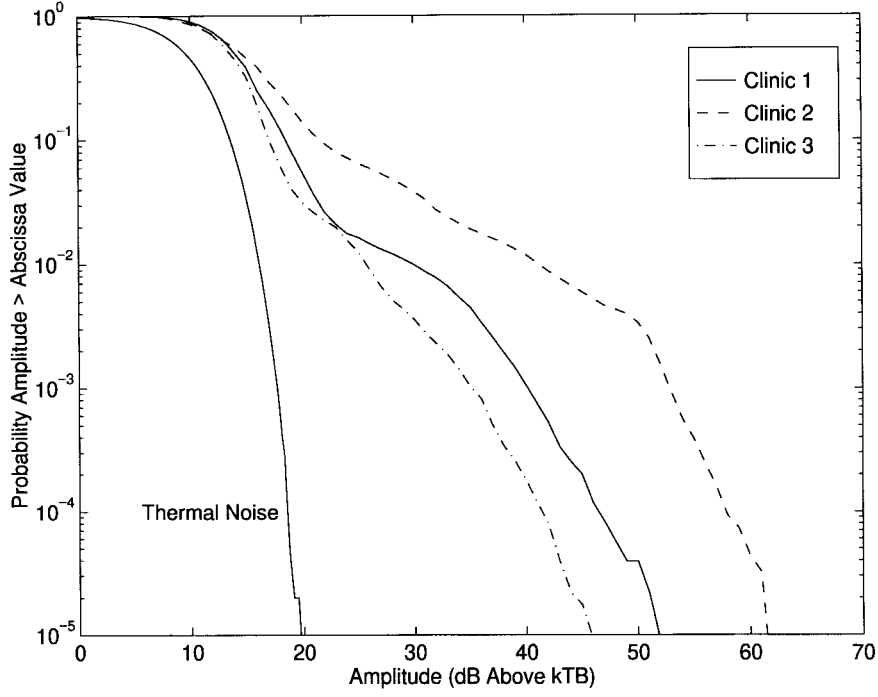


Fig. 10. The amplitude probability distribution  $APD(P_0)$  for individual clinic sites. The thermal noise distribution (labeled) is shown for comparison purposes.

which seemed to represent a more homogeneous statistical sample. The median impulsive noise amplitude, which is a reasonable approximation to the channel noise factor, was found to be 18.3 dB above the thermal noise floor in hospitals, while in clinics it was found to be 14.3 dB above the thermal noise floor. However, it was found that in clinics 99.99% of the impulsive noise was below a level which was 56.4 dB above the thermal noise floor, whereas in hospitals, 99.99%

of the impulsive noise was below a level which was 53.0 dB above the thermal noise floor.

The time characteristics of impulsive noise in clinics and hospitals were found to be similar. It was determined that, on average, impulsive noise bursts are separated by  $30 \mu$ s in both clinics and hospitals. Furthermore, in hospitals, 99.99% of consecutive noise bursts are separated by  $920 \mu$ s or less and, in clinics 99.99% of consecutive noise bursts are separated by

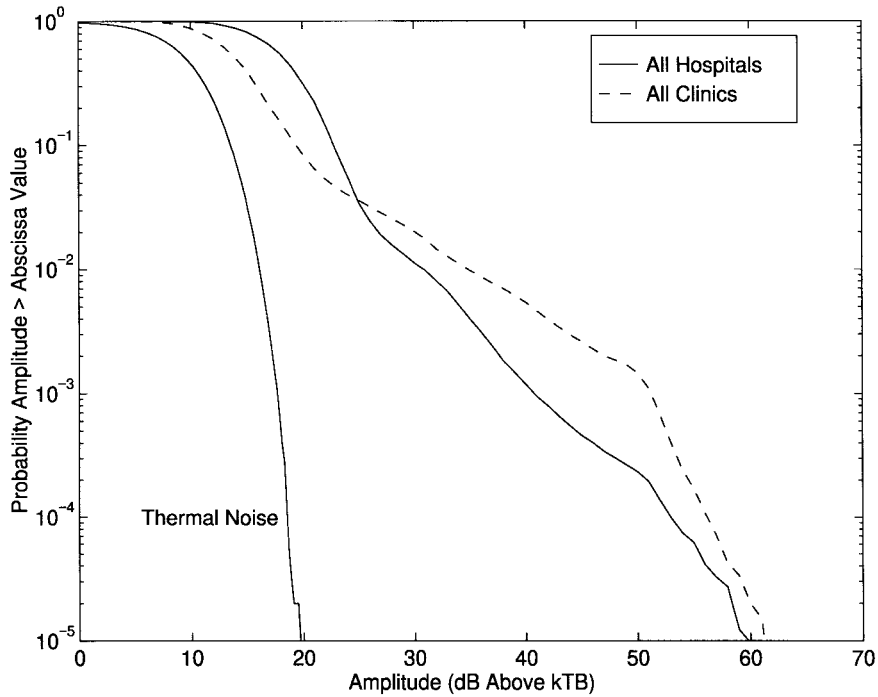


Fig. 11. The amplitude probability distribution  $APD(P_0)$  for all hospital sites and all clinic sites. The thermal noise distribution (labeled) is shown for comparison purposes.

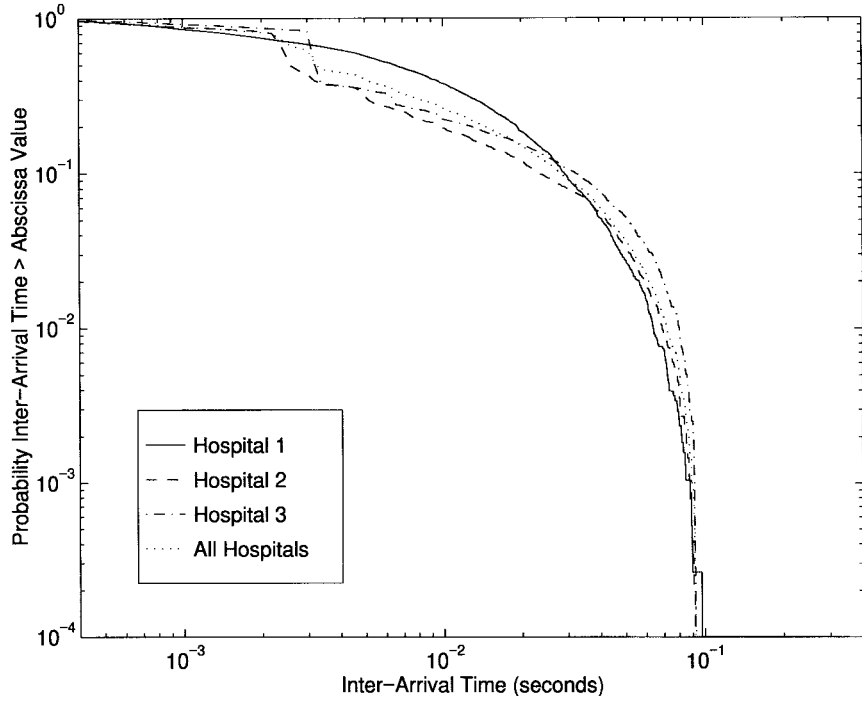


Fig. 12. The interarrival time distributions  $PSD(\tau_s)$  for the three individual hospital sites and for the combination of all hospital sites. The data were taken at system settings, which provided a minimum resolvable pulse duration of  $2 \mu\text{s}$ .

900  $\mu\text{s}$  or less. In both hospitals and clinics, on average, noise bursts have durations of  $2 \mu\text{s}$  or less. In hospitals, 99.99% of impulsive noise bursts last 190  $\mu\text{s}$  or less and, in clinics, 99.99% of impulsive noise bursts last 260  $\mu\text{s}$  or less.

By injecting large impulses of energy into radio receivers, impulsive noise is detrimental to wireless links. Such noise would cause "static" in voice systems or produce bit errors

in digital systems. In particular, noise that is repetitive in nature (such as presented in Fig. 6) has the potential to disrupt wireless communications for a significant period of time. The effects of impulsive noise can be mitigated by noise blanking circuits or by the choice of appropriate error correction codes in digital systems. The results presented here and in [5] have been used in the development of a software

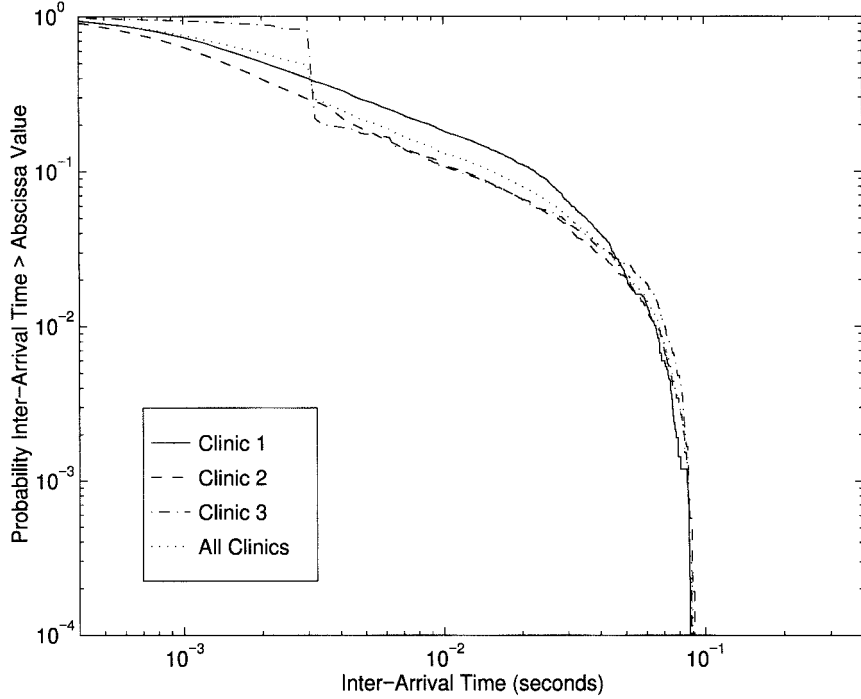


Fig. 13. The interarrival time distributions  $PSD(\tau_s)$  for the three individual clinic sites and for the combination of all clinic sites. The data were taken at system settings, which provided a minimum resolvable pulse duration of 2  $\mu$ s.

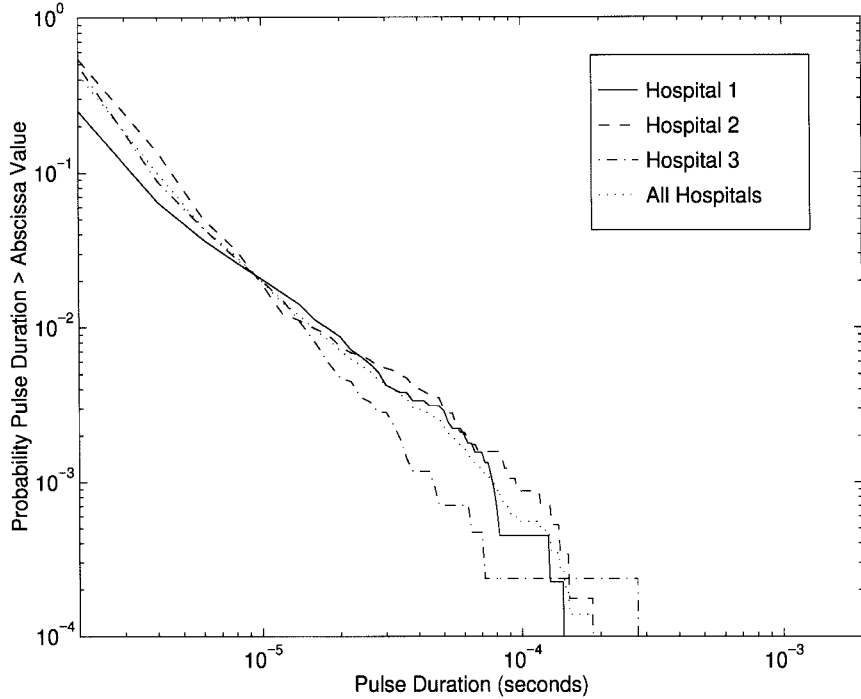


Fig. 14. The pulse duration distributions  $PDD(\tau_d)$  for the three individual hospital sites and for the combination of all hospital sites. The data were taken at system settings, which provided a minimum resolvable pulse duration of 2  $\mu$ s.

tool for realistic computer simulations of the propagation channel, which facilitates the design of wireless systems that are resistant to impulsive noise [13].

While the results presented here provide an understanding of the impulsive noise environment in three specific hospitals and three specific clinics, this empirically based field of research

merits further attention. For instance, dedicated investigations would facilitate the identification and detailed characterization of specific impulsive noise sources in hospitals and clinics. Also of benefit would be studies into the inherent polarization of impulsive noise since all the data analyzed in this report were taken using a vertically polarized antenna.

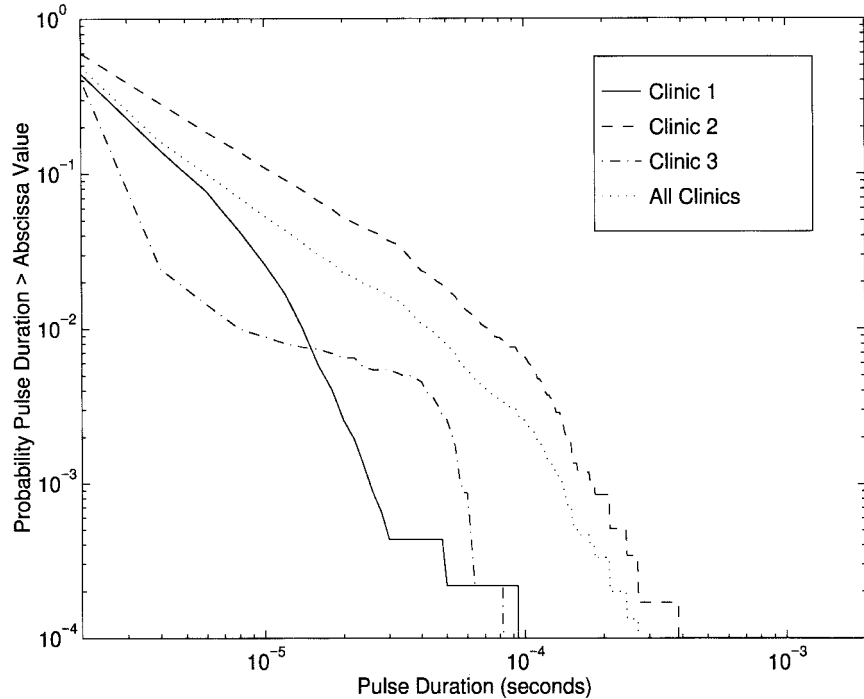


Fig. 15. The pulse duration distributions  $PDD(\tau_d)$  for the three individual clinic sites and for the combination of all clinic sites. The data were taken at system settings, which provided a minimum resolvable pulse duration of  $2 \mu\text{s}$ .

## REFERENCES

- [1] J. D. Parsons and J. G. Gardiner, *Mobile Communication Systems*. Glasgow, U.K.: Blackie, 1989.
- [2] R. A. Shepherd, "Measurements of amplitude probability distributions and power of automobile ignition noise at HF," *IEEE Trans. Veh. Technol.*, vol. VT-23, pp. 72-83, Aug. 1974.
- [3] G. L. Maxam, H. P. Hsu, and P. W. Wood, "Radiated ignition noise due to the individual cylinders of an automobile engine," *IEEE Trans. Veh. Technol.*, vol. VT-25, pp. 33-38, May 1976.
- [4] J. Y. C. Chia, "Interference characteristics of microwave ovens in indoor radio communications," IEEE 802.11 Tech. committee 11/91-52, May 1991.
- [5] K. L. Blackard, T. S. Rappaport, and C. W. Bostian, "Measurement and models of radio frequency impulsive noise for indoor wireless communications," *IEEE J. Selected Areas Commun.*, vol. 11, pp. 991-1001, Sept. 1993.
- [6] E. N. Skomal, *Man-Made Radio Noise*. New York: Van Nostrand Reinhold, 1978.
- [7] P. Vlach, B. Segal, and T. Pavlasek, "The measured & predicted electromagnetic environment at urban hospitals," in *Proc. IEEE Int. Symp. Electromagn. Compat.*, Atlanta, GA, Aug. 1995, pp. 4-7.
- [8] P. Boisvert, "The ambient electromagnetic environment in metropolitan hospitals," Master's thesis, Dept. Elect. Eng., McGill Univ., Montreal, Canada, 1991.
- [9] P. Vlach, "Measurement, prediction, and analysis of the radio frequency electromagnetic environment outside and inside hospitals," Master's thesis, Dept. Elect. Eng., McGill Univ., Montreal, Canada, 1994.
- [10] P. Boisvert, B. Segal, T. Pavlasek, S. Retfalvi, A. Sebe, and P. Caron, "Preliminary survey of the electromagnetic interference environment in hospitals," in *Proc. IEEE Int. Symp. Electromagn. Compat.*, Cherry Hill, NJ, Aug. 1991, pp. 214-219.
- [11] K. Foster, M. Soltys, S. Arnofsky, P. Doshi, D. Hanover, R. Mercado, D. Schleck, "Radio frequency field surveys in hospitals," *Biomed. Instrument. Technol.*, vol. 30, no. 2, pp. 155-159, Mar./Apr. 1996.
- [12] E. N. Skomal and A. A. Smith, *Measuring the Radio Frequency Environment*. New York: Van Nostrand Reinhold, 1985.
- [13] T. K. Blankenship, D. M. Krizman, and T. S. Rappaport, "Measurements and simulation of radio frequency impulsive noise in hospitals and clinics," in *Veh. Technol. Conf.*, Phoenix, AZ, May 1997, pp. 1942-1946.

**T. Keith Blankenship** (S'95) received the B.S. degree in applied mathematics from Virginia Commonwealth University, Richmond, in 1988, and the Ph.D. degree in physics from Virginia Tech, Blacksburg, in 1995. He is currently working toward the Master's degree in electrical engineering at Virginia Tech.

His current interests include radio receiver design, digital signal processing, and mobile radio propagation.

Dr. Blankenship was awarded the Phillip Morris Fellowship from Virginia Tech for his graduate study in physics. He is a member of Eta Kappa Nu.



**Theodore S. Rappaport** (S'83-M'87-SM'90) received the B.S.E.E., M.S.E.E., and Ph.D. degrees from Purdue University, West Lafayette, IN, in 1982, 1984, and 1987, respectively.

Since 1988, he has been on the Virginia Tech electrical and computer engineering faculty, where he is the James S. Tucker Professor and the Founder and Director of the Mobile & Portable Radio Research Group (MPRG—a university research and teaching center dedicated to the wireless communications field). In 1989 he founded TSR Technologies, Inc., Blacksburg, VA. He is President of Wireless Valley Communications, Inc., Blacksburg, VA. He has authored, co-authored, and co-edited nine books in the wireless field, including the popular textbook *Wireless Communications: Principles & Practice* (Englewood Cliffs, NJ: Prentice-Hall, 1996) and the compendia *Cellular Radio and Personal Communications: Selected Readings* and *Cellular Radio and Personal Communications: Advanced Selected Readings* (New York: IEEE Press, 1995 and 1996, respectively). He has co-authored more than 130 technical journal and conference papers and holds three patents.

Dr. Rappaport is active in the IEEE Communications and Vehicular Technology Societies. He is a registered Professional Engineer in the state of Virginia and is Fellow and past member of the board of directors of the Radio Club of America. He received the Marconi Young Scientist Award in 1990 and an NSF Presidential Faculty Fellowship in 1992. In 1996 he received honorable mention by Eta Kappa Nu for the G. Holmes MacDonald Outstanding Teaching Award. He serves on the editorial boards of the IEEE JOURNAL ON SELECTED AREAS IN COMMUNICATIONS and the *International Journal of Wireless Information Networks*.

